Acta Crystallographica Section B
Structural Science
ISSN 0108-7681

Nine isomeric nitrobenzylidene-iodoanilines: interplay of C—H···O hydrogen bonds, iodo···nitro interactions and aromatic $\pi\cdots\pi$ stacking interactions

Christopher Glidewell,[a]* R. Alan Howie,[b] John N. Low,[b]† Janet M. S. Skakle,[b] Solange M. S. V. Wardell[c] and James L. Wardell[d]

[a]School of Chemistry, University of St Andrews, St Andrews, Fife KY16 9ST, UK, [b]Department of Chemistry, University of Aberdeen, Meston Walk, Old Aberdeen AB24 3UE, UK, [c]Instituto de Química, Departamento de Química Orgânica, Universidade Federal Fluminense, 24020-150 Niterói, Rio de Janeiro-RJ, Brazil, and [d]Instituto de Química, Departamento de Química Inorgânica, Universidade Federal do Rio de Janeiro, CP 68563, 21945-970 Rio de Janeiro-RJ, Brazil

† Postal address: School of Engineering, University of Dundee, Dundee DD1 4HN, UK.

Correspondence e-mail: cg@st-andrews.ac.uk

Received 23 May 2002
Accepted 5 June 2002

Nine isomeric nitrobenzylidene-iodoanilines, $O_2NC_6H_4CH{=}NC_6H_4I$ [(I)–(IX)], have been synthesized and the structures of all except 4-nitrobenzylidene-4′-iodoaniline (IX) have been analyzed. 2-Nitrobenzylidene-2′-iodoaniline (I) contains isolated molecules, while 3-nitrobenzylidene-2′-iodoaniline (II) and 2-nitrobenzylidene-3′-iodoaniline (IV) both contain chains of molecules linked by C—H···O hydrogen bonds: similar chains in 4-nitrobenzylidene-2′-iodoaniline (III) are further linked by aromatic $\pi\cdots\pi$ stacking interactions, forming sheets. In both 3-nitrobenzylidene-3′-iodoaniline and 4-nitrobenzylidene-3′-iodoaniline, (V) and (VI), a combination of C—H···O hydrogen bonds and iodo···nitro interactions generates molecular ladders that are linked into sheets by aromatic $\pi\cdots\pi$ stacking interactions, while in 2-nitrobenzylidene-4′-iodoaniline and 3-nitrobenzylidene-4′-iodoaniline, (VII) and (VIII), which both crystallize with $Z' = 2$ in $C2/c$ and $P\bar{1}$, respectively, the combination of C—H···O hydrogen bonds and iodo···nitro interactions generates sheets, which in (VIII) are further linked by $\pi\cdots\pi$ stacking interactions to form a three-dimensional structure. The 4,4′-isomer (IX) crystallizes in $Fdd2$ with $Z' = 2$, but both molecules are intractably disordered.

1. Introduction

We recently reported the molecular and supramolecular structures of a number of iodo-nitroarenesulfonamides $O_2NC_6H_4NHSO_2C_6H_4I$ (Kelly *et al.*, 2002): in these systems, the supramolecular structures display a very wide range of aggregation patterns, reflecting the subtle interplay of N—H···O and C—H···O hydrogen bonds (where the acceptors can, in general, be either in the nitro groups or in the sulfonamide units) in competition with the iodo···nitro and aromatic $\pi\cdots\pi$ stacking interactions. In order to simplify the range of possible intermolecular interactions, we have now turned to a related series of iodo-nitro species, the nitrobenzylidene-iodoanilines, $O_2NC_6H_4CH{=}NC_6H_4I$ (Scheme 1), which have been specifically selected to preclude the possible occurrence of the comparatively strong N—H···O hydrogen bonds, so leaving the three weaker interactions as the major determinants of the supramolecular structures. All nine isomers [2-nitrobenzylidene-2′-iodoaniline (I), 3-nitrobenzylidene-2′-iodoaniline (II), 4-nitrobenzylidene-2′-iodoaniline (III), 2-nitrobenzylidene-3′-iodoaniline (IV), 3-nitrobenzylidene-3′-iodoaniline (V), 4-nitrobenzylidene-3′-iodoaniline (VI), 2-nitrobenzylidene-4′-iodoaniline (VII), 3-nitrobenzylidene-4′-iodoaniline (VIII) and 4-nitrobenzylidene-4′-iodoaniline (IX)] have been synthesized, and we present here an analysis of the various interactions present in their crystal structures.

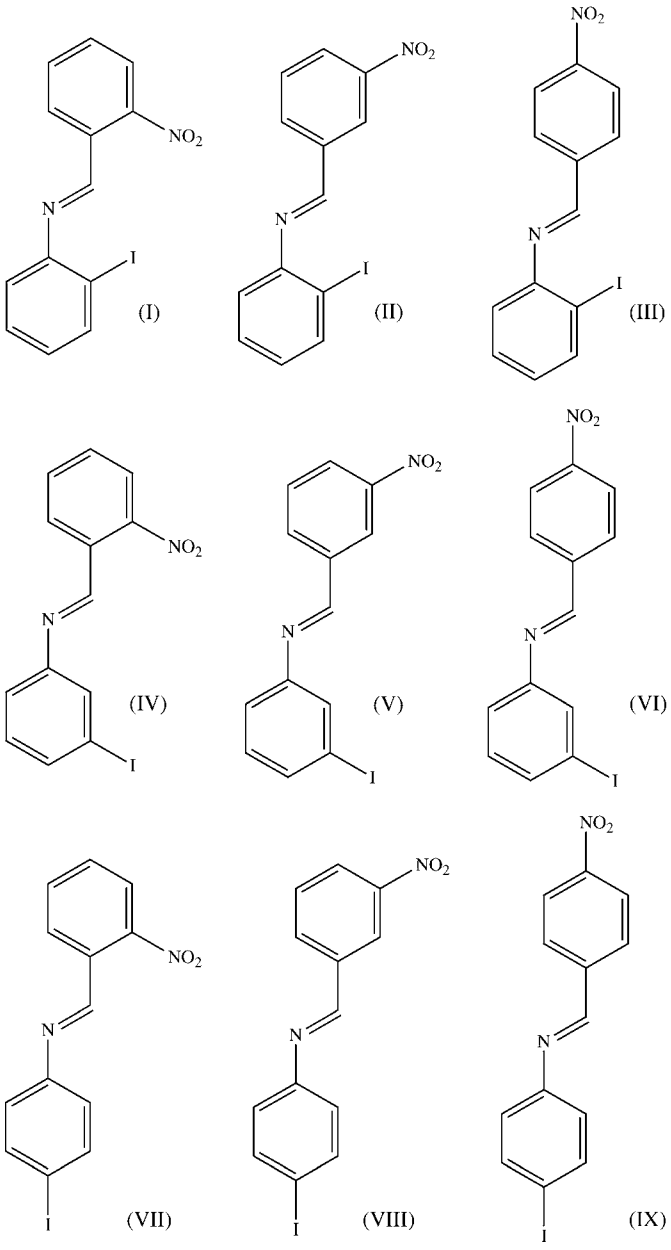

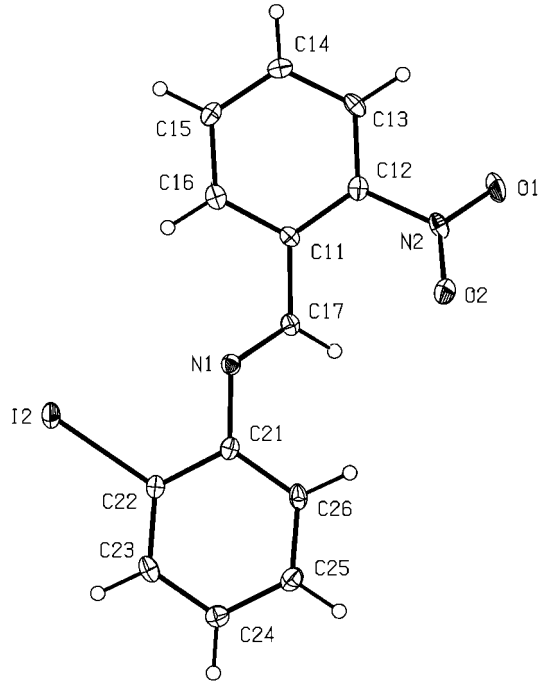

Figure 1
A molecule of (I) showing the atom-labelling scheme. Displacement ellipsoids are drawn at the 30% probability level.

2. Experimental

2.1. Synthesis

Samples of (I)–(IX) were all prepared by condensation of the appropriate nitrobenzaldehydes and iodoanilines: crystals of (I)–(VIII) suitable for single-crystal X-ray diffraction were grown by slow evaporation of solutions in ethanol. For (IX), many crystallization solvents were investigated: the only material usable for diffraction study was obtained from a solution in carbon tetrachloride.

2.2. Data collection, structure solution and refinement

Diffraction data for (I)–(IX) were collected at 120 (2) K using a Nonius KappaCCD diffractometer with graphite-monochromated Mo $K\alpha$ radiation ($\lambda = 0.71073$ Å). Other details of cell data, data collection and data refinement are summarized in Table 1, together with details of the software employed (Ferguson, 1999; Nonius, 1997; Otwinowski & Minor, 1997; Sheldrick, 1997*a*,*b*; Spek, 2002).

For (I) the space group $P2_1/n$ was uniquely assigned from the systematic absences, and space group $P2_1/c$ was similarly assigned for each of (II)–(IV). Space group $P2_12_12_1$ was uniquely assigned for (V) and (VI), and their absolute structures were determined by refinement of the Flack parameters (Flack, 1983): the refined values were −0.03 (4) and −0.07 (3), respectively, and 1141 and 1023 Friedel pairs were present. The systematic absences for (VII) permitted $C2/c$ and Cc as possible space groups: $C2/c$ was selected and was confirmed by the subsequent analysis. Compound (VIII) is triclinic: space group $P\bar{1}$ was selected and confirmed by the analysis. For (IX), the space group $Fdd2$ was uniquely assigned from the systematic absences, and the unit-cell dimensions, $a = 16.4311$ (17), $b = 39.469$ (3), $c = 14.9002$ (1) Å, are consistent with $Z = 32$ (*i.e.* $Z' = 2$). However, both of the independent molecules were found to be intractably disordered and repeated attempts to model this disorder and then to refine the structure proved fruitless. The structures were solved by direct methods and refined with all data on F^2. A weighting scheme based on $P = [F_o^2 + 2F_c^2]/3$ was employed in order to reduce statistical bias (Wilson, 1976). All H atoms were located from difference maps and were included in the refinements as riding atoms with a C—H distance of 0.95 Å.

Supramolecular analyses were made with the aid of *PLATON* (Spek, 2002). Details of molecular conformations, the C—H···O interactions and the iodo···nitro interactions

Table 1
Experimental details.

	(I)	(II)	(III)	(IV)
Crystal data				
Chemical formula	$C_{13}H_9IN_2O_2$	$C_{13}H_9IN_2O_2$	$C_{13}H_9IN_2O_2$	$C_{13}H_9IN_2O_2$
Chemical formula weight	352.12	352.12	352.12	352.12
Cell setting, space group	Monoclinic, $P2_1/n$	Monoclinic, $P2_1/c$	Monoclinic, $P2_1/c$	Monoclinic, $P2_1/c$
a, b, c (Å)	8.0664 (4), 10.7191 (5), 14.5692 (9)	7.9059 (3), 22.6230 (7), 7.6095 (2)	10.1401 (7), 13.7454 (10), 9.7829 (6)	12.0589 (6), 4.5562 (2), 22.9725 (14)
β (°)	99.026 (2)	113.755 (1)	113.961 (4)	97.3970 (18)
V (Å^3)	1244.12 (11)	1245.69 (7)	1246.03 (15)	1251.67 (11)
Z	4	4	4	4
D_x (Mg m^{-3})	1.880	1.878	1.877	1.869
Radiation type	Mo $K\alpha$	Mo $K\alpha$	Mo $K\alpha$	Mo $K\alpha$
No. of reflections for cell parameters	2777	2685	2829	2731
θ range (°)	3.11–27.48	2.96–27.46	2.96–27.49	3.41–27.48
μ (mm^{-1})	2.569	2.565	2.565	2.553
Temperature (K)	120 (2)	120 (2)	120 (2)	120 (2)
Crystal form, colour	Lath, brown	Block, brown	Block, yellow	Needle, orange
Crystal size (mm)	0.17 × 0.04 × 0.02	0.25 × 0.20 × 0.10	0.15 × 0.08 × 0.07	0.50 × 0.10 × 0.05
Data collection				
Diffractometer	KappaCCD	KappaCCD	KappaCCD	KappaCCD
Data collection method	φ scans, and ω scans with κ offsets	φ scans, and ω scans with κ offsets	φ scans, and ω scans with κ offsets	φ scans, and ω scans with κ offsets
Absorption correction	Multi-scan	Multi-scan	Multi-scan	Multi-scan
T_{min}	0.929	0.599	0.641	0.763
T_{max}	0.950	0.774	0.836	0.876
No. of measured, independent and observed reflections	7432, 2777, 1865	11972, 2685, 2327	7436, 2829, 1954	5744, 2731, 2033
Criterion for observed reflections	$I > 2\sigma(I)$	$I > 2\sigma(I)$	$I > 2\sigma(I)$	$I > 2\sigma(I)$
R_{int}	0.0569	0.0792	0.0768	0.0388
θ_{max} (°)	27.48	27.46	27.49	27.48
Range of h, k, l	$-10 \rightarrow h \rightarrow 9$ $-12 \rightarrow k \rightarrow 13$ $-18 \rightarrow l \rightarrow 18$	$-10 \rightarrow h \rightarrow 10$ $-29 \rightarrow k \rightarrow 29$ $-9 \rightarrow l \rightarrow 8$	$-11 \rightarrow h \rightarrow 13$ $-16 \rightarrow k \rightarrow 17$ $-12 \rightarrow l \rightarrow 9$	$-13 \rightarrow h \rightarrow 15$ $-4 \rightarrow k \rightarrow 5$ $-23 \rightarrow l \rightarrow 29$
Refinement				
Refinement on	F^2	F^2	F^2	F^2
$R[F^2 > 2\sigma(F^2)]$, $wR(F^2)$, S	0.0401, 0.0736, 0.982	0.0385, 0.1012, 1.067	0.0423, 0.0981, 1.005	0.032, 0.0627, 0.945
No. of reflections and parameters used in refinement	2777, 163	2685, 163	2829, 163	2731, 163
H-atom treatment	H-atom parameters constrained	H-atom parameters constrained	H-atom parameters constrained	H-atom parameters constrained
Weighting scheme	$w = 1/[\sigma^2(F_o^2) + (0.005P)^2]$ where $P = (F_o^2 + 2F_c^2)/3$	$w = 1/[\sigma^2(F_o^2) + (0.0409P)^2 + 3.5014P]$ where $P = (F_o^2 + 2F_c^2)/3$	$w = 1/[\sigma^2(F_o^2) + (0.0352P)^2]$ where $P = (F_o^2 + 2F_c^2)/3$	$w = 1/[\sigma^2(F_o^2) + (0.0136P)^2]$ where $P = (F_o^2 + 2F_c^2)/3$
$(\Delta/\sigma)_{max}$	0.001	0.000	0.000	0.000
$\Delta\rho_{max}$, $\Delta\rho_{min}$ (e Å^{-3})	1.068, −1.011	1.442, −1.249	0.97, −1.428	0.974, −0.967

	(V)	(VI)	(VII)	(VIII)
Crystal data				
Chemical formula	$C_{13}H_9IN_2O_2$	$C_{13}H_9IN_2O_2$	$C_{13}H_9IN_2O_2$	$C_{13}H_9IN_2O_2$
Chemical formula weight	352.12	352.12	352.12	352.12
Cell setting, space group	Orthorhombic, $P2_12_12_1$	Orthorhombic, $P2_12_12_1$	Monoclinic, C_2/c	Triclinic, $P\overline{1}$
a, b, c (Å)	7.4741 (3), 11.3487 (4), 14.2039 (6)	7.1179 (2), 12.3905 (3), 13.6983 (5)	52.458 (2), 4.3786 (2), 23.5973 (13)	7.2646 (1), 11.8251 (2), 15.0057 (3)
α, β, γ (°)	90	90, 90, 90	90, 114.185 (2), 90	103.2458 (6), 98.3999 (7), 91.6291 (10)
V (Å^3)	1204.79 (8)	1208.11 (6)	4944.4 (4)	1238.74 (4)
Z	4	4	16	4
D_x (Mg m^{-3})	1.941	1.936	1.892	1.888
Radiation type	Mo $K\alpha$	Mo $K\alpha$	Mo $K\alpha$	Mo $K\alpha$
No. of reflections for cell parameters	2752	2627	5417	5602
θ range (°)	3.08–27.49	2.97–27.47	3.02–27.48	2.96–27.51
μ (mm^{-1})	2.653	2.645	2.585	2.580
Temperature (K)	120 (2)	120 (2)	120 (2)	120 (2)
Crystal form, colour	Needle, colourless	Block, yellow	Needle, yellow	Rod, yellow

Table 1 (continued)

	(V)	(VI)	(VII)	(VIII)
Crystal size (mm)	0.20 × 0.06 × 0.06	0.20 × 0.10 × 0.10	0.15 × 0.04 × 0.03	0.28 × 0.10 × 0.08
Data collection				
Diffractometer	KappaCCD	KappaCCD	KappaCCD	KappaCCD
Data collection method	φ scans, and ω scans with κ offsets	φ scans, and ω scans with κ offsets	φ scans, and ω scans with κ offsets	φ scans, and ω scans with κ offsets
Absorption correction	Multi-scan	Multi-scan	Multi-scan	Multi-scan
T_{min}	0.665	0.607	0.893	0.587
T_{max}	0.853	0.768	0.928	0.814
No. of measured, independent and observed reflections	8100, 2752, 2275	6019, 2627, 2453	13621, 5417, 2368	18561, 5602, 4991
Criterion for observed reflections	$I > 2\sigma(I)$	$I > 2\sigma(I)$	$I > 2\sigma(I)$	$I > 2\sigma(I)$
R_{int}	0.1173	0.0334	0.1280	0.0757
θ_{max} (°)	27.49	27.47	27.48	27.51
Range of h, k, l	$-9 \rightarrow h \rightarrow 8$ $-13 \rightarrow k \rightarrow 14$ $-18 \rightarrow l \rightarrow 16$	$-8 \rightarrow h \rightarrow 7$ $-16 \rightarrow k \rightarrow 13$ $-17 \rightarrow l \rightarrow 15$	$-67 \rightarrow h \rightarrow 67$ $-5 \rightarrow k \rightarrow 5$ $-30 \rightarrow l \rightarrow 30$	$-9 \rightarrow h \rightarrow 9$ $-15 \rightarrow k \rightarrow 15$ $-19 \rightarrow l \rightarrow 19$
Refinement				
Refinement on	F^2	F^2	F^2	F^2
$R[F^2 > 2\sigma(F^2)]$, $wR(F^2)$, S	0.0475, 0.1003, 1.003	0.0288, 0.0783, 1.11	0.0594, 0.0986, 0.839	0.0299, 0.0769, 1.026
No. of reflections and parameters used in refinement	2752, 163	2627, 163	5417, 325	5602, 325
H-atom treatment	H-atom parameters constrained	H-atom parameters constrained	H-atom parameters constrained	H-atom parameters constrained
Weighting scheme	$w = 1/[\sigma^2(F_o^2) + (0.0287P)^2]$ where $P = (F_o^2 + 2F_c^2)/3$	$w = 1/[\sigma^2(F_o^2) + (0.0355P)^2 + 0.6144P]$ where $P = (F_o^2 + 2F_c^2)/3$	$w = 1/[\sigma^2(F_o^2) + (0.01P)^2]$ where $P = (F_o^2 + 2F_c^2)/3$	$w = 1/[\sigma^2(F_o^2) + (0.0279P)^2 + 1.1231P]$ where $P = (F_o^2 + 2F_c^2)/3$
$(\Delta/\sigma)_{max}$	0.001	0.001	0.001	0.003
$\Delta\rho_{max}$, $\Delta\rho_{min}$ (e Å^{-3})	2.027, −1.519	0.687, −1.08	1.228, −0.946	0.656, −1.175

Computer programs used: *PRPKAPPA* (Ferguson, 1999), *KappaCCD Server Software* (Nonius, 1997), *DENZO-SMN* (Otwinowski & Minor, 1997), *SHELXL*97 (Sheldrick, 1997*a*), *SHELXS*97 (Sheldrick, 1997*b*), *PLATON* (Spek, 2002).

are given in Tables 2–4, respectively.[1] The diagrams were prepared with the aid of *PLATON* (Spek, 2002). Figs. 1–8 show the individual molecular species in (I)–(VIII) with the atom-labelling schemes, and Figs. 9–23 show aspects of their supramolecular structures.

3. Molecular conformations and dimensions

In each compound, the central C—N═CH—C fragment is effectively planar. This unit then provides a convenient reference frame for the definition of the overall skeletal conformation in terms of the torsional angles defining the rotations of the two independent rings out of this plane (Table 2). Since the two edges of the central fragment are distinguishable, as the one edge carries a C—H bond and the other edge carries a lone pair at N, this unit also provides a reference against which to define the location of iodo or nitro substituents in *ortho* or *meta* positions.

Thus, for example, in (I) (Fig. 1) the iodo and nitro substituents are on opposite edges of the molecule, while in (II) (Fig. 2) they are on the same edge. Again, although (V) and (VI) both crystallize in space group $P2_12_12_1$, the 3-iodo

Table 2
Molecular conformations.

	Framework torsional angles (°)	
	N1—C17—C11—C12	C17—N1—C21—C22
(I)	156.9 (4)	−150.7 (4)
(II)	14.0 (7)	146.3 (5)
(III)	178.9 (4)	−135.6 (5)
(IV)	157.6 (3)	−40.3 (4)
(V)	−175.9 (6)	−143.4 (6)
(VI)	166.5 (5)	39.9 (7)
(VII)	−156.6 (8)†	31.1 (13)‡
	−153.6 (8)§	−40.6 (12)¶
(VIII)	177.2 (3)†	3.4 (4)‡
	19.2 (4)§	166.1 (3)¶

	Dihedral angles involving nitro groups (°)	
(I)	(C11—C16)^(O1, O2, N2, C12)	26.6 (2)
(II)	(C11—C16)^(O1, O2, N3, C13)	1.2 (3)
(III)	(C11—C16)^(O1, O2, N4, C14)	12.5 (3)
(IV)	(C11—C16)^(O1, O2, N2, C12)	30.0 (2)
(V)	(C11—C16)^(O1, O2, N3, C13)	9.0 (4)
(VI)	(C11—C16)^(O1, O2, N4, C14)	2.5 (3)
(VII)	(C11—C16)^(O11, O12, N12, C12)	25.4 (5)
	(C31—C36)^(O31, O32, N32, C32)	23.1 (5)
(VIII)	(C11—C16)^(O11, O12, N13, C13)	8.9 (2)
	(C31—C36)^(O31, O32, N33, C33)	13.8 (2)

† N11—C17—C11—C12. ‡ C17—N11—C21—C22. § N21—C37—C31—C32. ¶ C37—N21—C41—C42.

[1] Lists of atomic coordinates, anisotropic displacement parameters, geometric parameters and structure factors have been deposited with the IUCr (Reference NA0138). Services for accessing these data are described at the back of the journal.

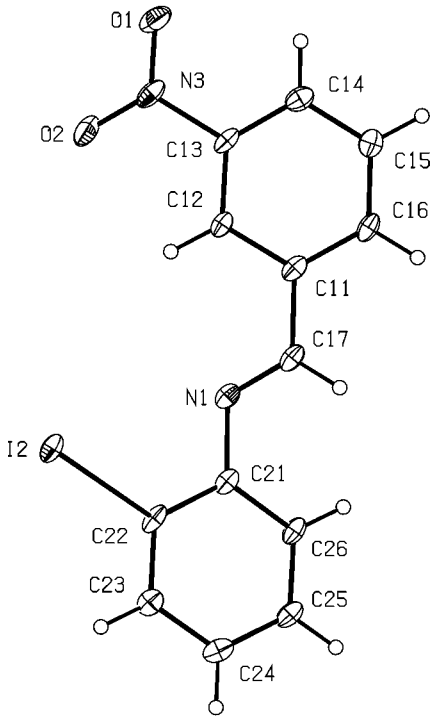

Figure 2
A molecule of (II) showing the atom-labelling scheme. Displacement ellipsoids are drawn at the 30% probability level.

substituent in (V) (Fig. 5) is on the edge opposite the C17—H17 bond, while in (VI) (Fig. 6) it is on the same edge. Perhaps most strikingly, in (VIII) (Fig. 8) the two independent molecules have the nitro substituents on different edges relative to the reference C—H bond: in molecule 1, the nitro group is on the same edge as this C—H bond, while in molecule 2 the nitro group is on the opposite edge.

For nitroarenes, the minimum energy conformation generally has the nitro group coplanar with the adjacent arene ring, although the barrier to rotation about the connecting C—N bond is usually small (Domenicano *et al.*, 1990). Thus a nitro group can readily be rotated out of the plane of the adjacent arene ring by either intra- or intermolecular interactions involving the O atoms of the nitro groups: both hydrogen bonds and I···O interactions can contribute to this perturbation. The data in Table 2 indicate that the biggest nitro-group rotations are apparent in (I), (IV) and (VII), namely the three compounds containing 2-nitro groups. In each of these examples, the nitro group is on the edge of the molecule closest to the C—H bond in the central spacer unit, and in (I) and (VII) it is tempting to associate the nitro-group rotation with a repulsive intramolecular H···O contact.

Table 4
Geometrical parameters for iodo···nitro interactions in compounds (V)–(VIII) (Å, °).

		I···O	C—I···O	I···O—N
(V)	C123—I3···O2^{i}	3.104 (4)	153.8 (2)	117.0 (3)
(VI)	C23—I3···O1^{i}	3.219 (3)	162.0 (2)	162.8 (3)
(VII)	C44—I24···O12^{ii}	3.585 (6)	87.8 (3)	143.1 (5)
(VIII)	C24—I14···O32^{iii}	3.242 (2)	163.9 (2)	147.5 (2)
	C44—I24···O12^{iv}	3.222 (2)	171.6 (2)	151.8 (2)

Symmetry codes: (i) $x, y, 1+z$; (ii) $x, 2-y, -\frac{1}{2}+z$; (iii) $2-x, -y, 2-z$; (iv) $1-x, 2-y, 1-z$.

4. Supramolecular structures

The supramolecular structures of (I)–(IX) are characterized by a combination of C—H···O hydrogen bonds, two-centre iodo···nitro interactions and aromatic $\pi\cdots\pi$ stacking interactions (Tables 3 and 4). To codify the hydrogen-bonding motifs we employ the now-familiar graph-set notation (Etter, 1990; Bernstein *et al.*, 1995; Motherwell *et al.*, 1999), and for the iodo···nitro interactions we employ the recently described (Starbuck *et al.*, 1999) extension of this notation to encompass secondary bonding, wherein we regard the negatively polarized O atoms of the nitro group as 'donors' and the positively polarized I atoms as 'acceptors'.

4.1. Zero-dimensional structures (isolated molecules)

In (I) (Fig. 1), there are neither intermolecular C—H···O hydrogen bonds nor any iodo···nitro interactions, although an

Table 3
Hydrogen-bonding geometry and short intramolecular contacts (Å, °).

	D—H···A	H···A	D···A	D—H···A	Motif	Direction
(I)	C17—H17···O2	2.37	2.723 (5)	102	$S(6)$	–
(II)	C17—H17···O2^{i}	2.60	3.538 (6)	172	$C(7)$	[101]
	C26—H26···O2^{i}	2.59	3.286 (6)	131	$C(10)$	[101]
(III)	C13—H13···O1^{ii}	2.44	3.331 (6)	156	$C(5)$	[001]
(IV)	C22—H22···O1^{iii}	2.45	3.397 (4)	174	$C(9)$	[010]
(V)	C16—H16···O1^{iv}	2.58	3.437 (8)	151	$C(7)$	[001]
(VI)	C22—H22···O2^{iv}	2.56	3.487 (6)	166	$C(11)$	[001]
(VII)	C13—H13···O31	2.46	3.140 (11)	129	D	–
	C17—H17···O12	2.34	2.742 (13)	105	$S(6)$	–
	C37—H37···O31	2.28	2.700 (11)	106	$S(6)$	–
	C33—H33···O32^{v}	2.47	3.370 (12)	158	$R_2^2(10)$	–
	C34—H34···O11^{vi}	2.57	3.327 (12)	137	$R_4^4(22)$	–
(VIII)	C17—H17···O31	2.43	3.303 (3)	153	D	–
	C37—H37···O11^{vii}	2.53	3.406 (3)	154	$R_4^4(28)$	–

Symmetry codes: (i) $1+x, y, 1+z$; (ii) $x, \frac{3}{2}-y, -\frac{1}{2}+z$; (iii) $1-x, -\frac{1}{2}+y, \frac{1}{2}-z$; (iv) $\frac{1}{2}-x, 1-y, \frac{1}{2}+z$; (v) $1-x, -1-y, 1-z$; (vi) $1-x, -y, 1-z$; (vii) $1-x, 1-y, 1-z$.

intramolecular hydrogen bond is present (Table 3): furthermore, aromatic $\pi\cdots\pi$ stacking interactions are also absent, so that the structure of (I) must be regarded as comprising isolated molecules.

4.2. One-dimensional structures

4.2.1. Simple chains. In (IV) (Fig. 4), the molecules are linked into spiral chains by means of a single C—H$\cdots$O hydrogen bond (Table 3). Atom C22 at (x, y, z) acts as hydrogen-bond donor to nitro O1 at ($1-x$, $-\frac{1}{2}+y$, $\frac{1}{2}-z$), while C22 at ($1-x$, $-\frac{1}{2}+y$, $\frac{1}{2}-z$) in turn acts as donor to O1 at (x, $-1+y$, z), so producing a $C(9)$ chain running parallel to the [010] direction and generated by the 2_1 screw axis along ($\frac{1}{2}$, y, $\frac{1}{4}$) (Fig. 9). A second antiparallel chain, related to the first by the action of the inversion centres, is generated by the 2_1 axis along ($\frac{1}{2}$, $-y$, $\frac{3}{4}$). There are neither iodo$\cdots$nitro interactions nor aromatic $\pi\cdots\pi$ stacking interactions between adjacent chains.

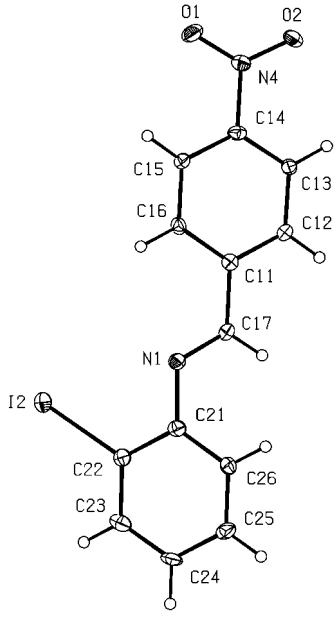

Figure 3
A molecule of (III) showing the atom-labelling scheme. Displacement ellipsoids are drawn at the 30% probability level.

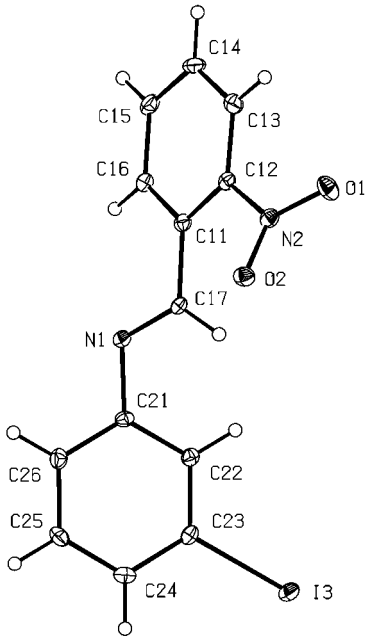

Figure 4
A molecule of (IV) showing the atom-labelling scheme. Displacement ellipsoids are drawn at the 30% probability level.

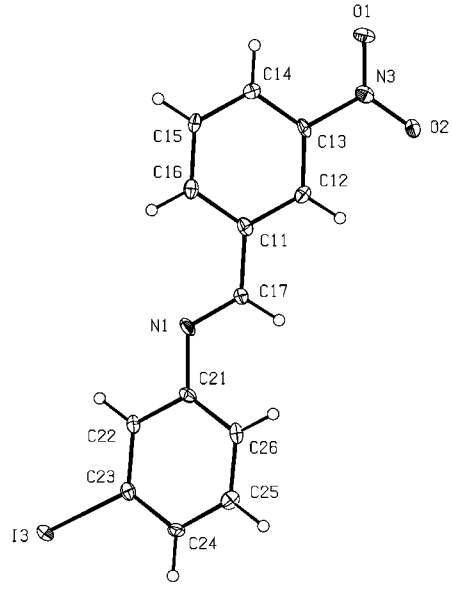

Figure 5
A molecule of (V) showing the atom-labelling scheme. Displacement ellipsoids are drawn at the 30% probability level.

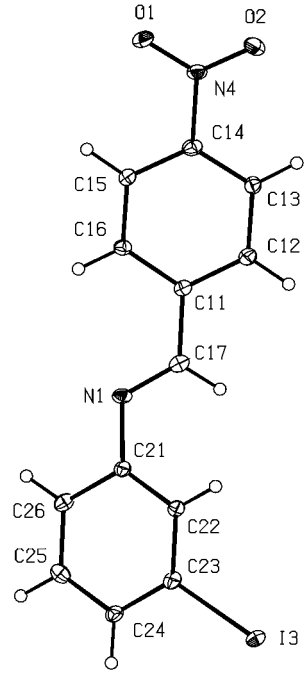

Figure 6
A molecule of (VI) showing the atom-labelling scheme. Displacement ellipsoids are drawn at the 30% probability level.

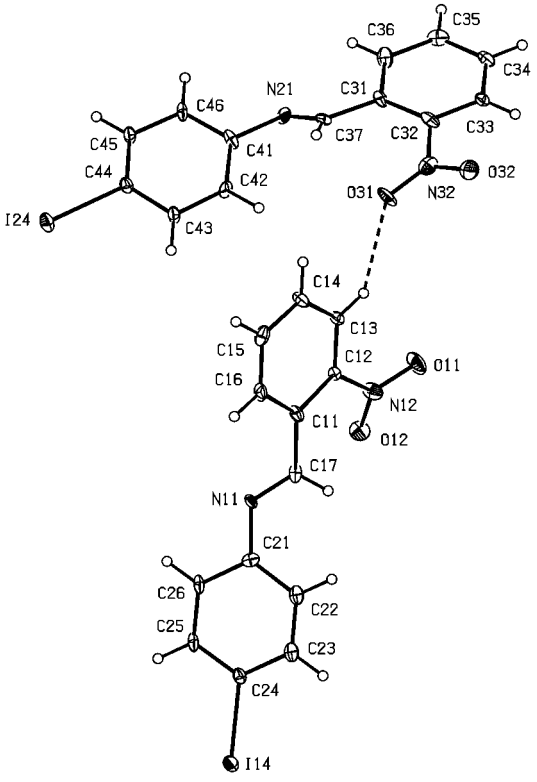

Figure 7
The two independent molecules of (VII) showing the atom-labelling scheme. Displacement ellipsoids are drawn at the 30% probability level.

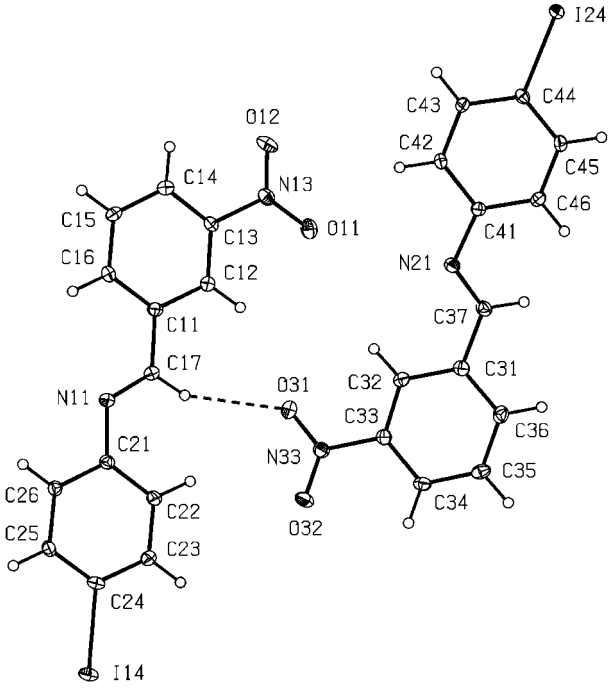

Figure 8
The two independent molecules of (VIII) showing the atom-labelling scheme. Displacement ellipsoids are drawn at the 30% probability level.

4.2.2. A chain of rings. There are two weak intermolecular C—H···O hydrogen bonds in the structure of (II) (Fig. 2, Table 3), and these link the molecules into a chain of rings (Bernstein *et al.*, 1995). Atoms C17 and C26 in the molecule at (x, y, z) both act as hydrogen-bond donors to O2 in the molecule at ($1 + x$, y, $1 + z$), so generating by translation a $C(7)$ and $C(10)$ chain, respectively, running parallel to the [101] direction: the combined effect of these two hydrogen bonds is the formation of an $R_2^1(7)$ ring, so that the complete

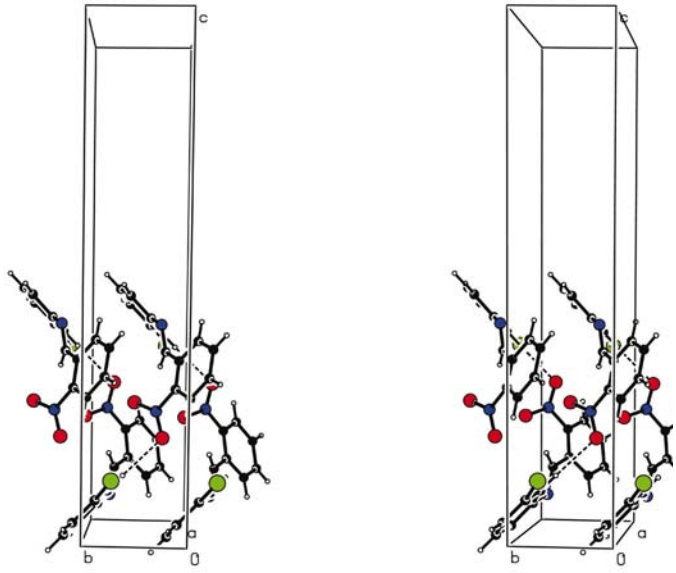

Figure 9
Stereoview of part of the crystal structure of (IV) showing the formation of a spiral chain around the screw axis along ($\frac{1}{2}$, y, $\frac{1}{4}$).

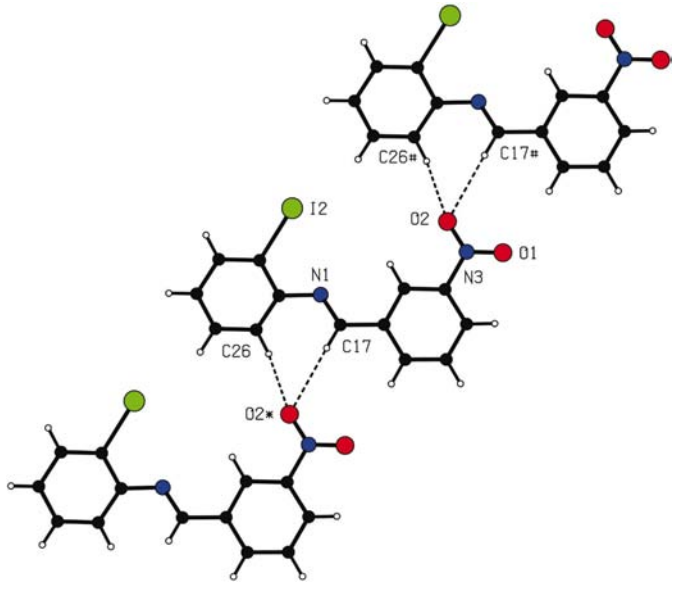

Figure 10
Part of the crystal structure of (II) showing the formation of a chain of rings along [101]. For the sake of clarity, the unit-cell box is omitted. The atoms marked with a star (*) or hash (#) are at the symmetry positions ($1 + x$, y, $1 + z$) and ($-1 + x$, y, $-1 + z$), respectively.

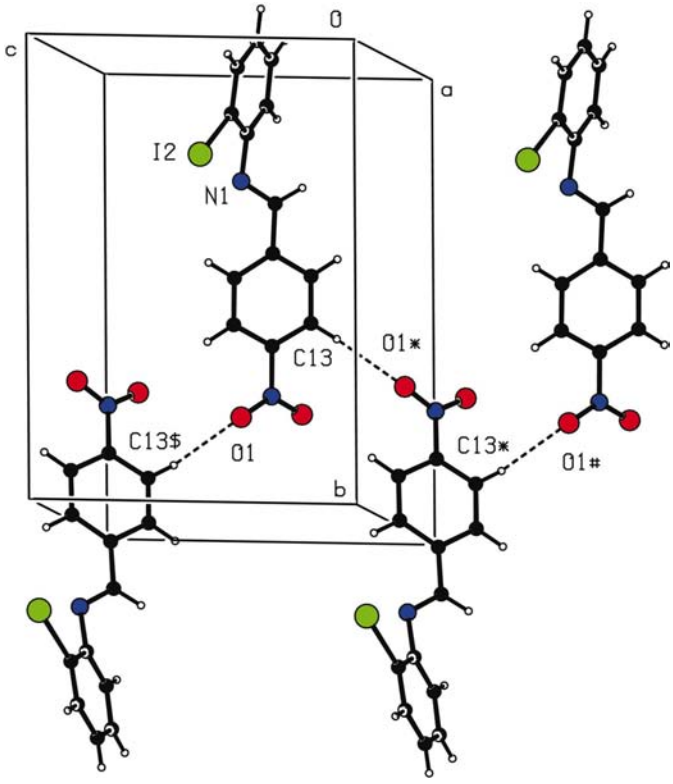

Figure 11
Part of the crystal structure of (III) showing the formation of a zigzag chain along [001]. The atoms marked with a star (*), hash (#) or dollar sign ($) are at the symmetry positions $(x, \frac{3}{2} - y, -\frac{1}{2} + z)$, $(x, y, -1 + z)$ and $(x, \frac{3}{2} - y, \frac{1}{2} + z)$, respectively.

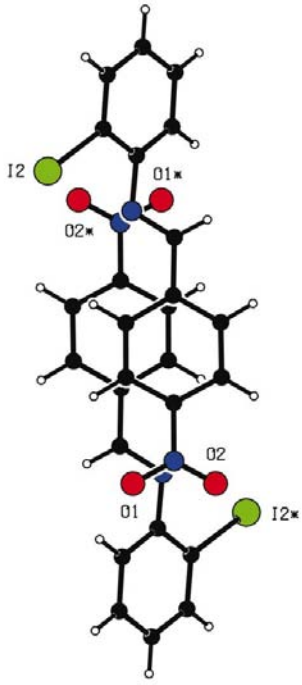

Figure 12
Part of the crystal structure of (III) showing the centrosymmetric $\pi\cdots\pi$ stacking interaction. The atoms marked with a star (*) are at the symmetry position $(1 - x, 1 - y, 1 - z)$.

descriptor of the hydrogen bonding is $C(7)C(10)[R_2^1(7)]$ (Fig. 10). There are neither iodo···nitro interactions nor aromatic $\pi\cdots\pi$ stacking interactions between adjacent chains.

4.3. Two-dimensional structures

4.3.1. Hydrogen-bonded chains linked into sheets by $\pi\cdots\pi$ interactions. Molecules of (III) are linked into chains by a single C—H···O hydrogen bond (Table 3), and the chains are linked into sheets by means of aromatic $\pi\cdots\pi$ stacking interactions, but there are no iodo···nitro interactions present. Atom C13 at (x, y, z) acts as hydrogen-bond donor to O1 at $(x, \frac{3}{2} - y, -\frac{1}{2} + z)$, and C13 at $(x, \frac{3}{2} - y, -\frac{1}{2} + z)$ likewise acts as donor to O1 at $(x, y, -1 + z)$. In this way, a $C(5)$ chain parallel to [001] is generated by the *c*-glide plane at $y = 0.75$ (Fig. 11), and a similar but antiparallel chain is generated by the *c*-glide plane at $y = 0.25$.

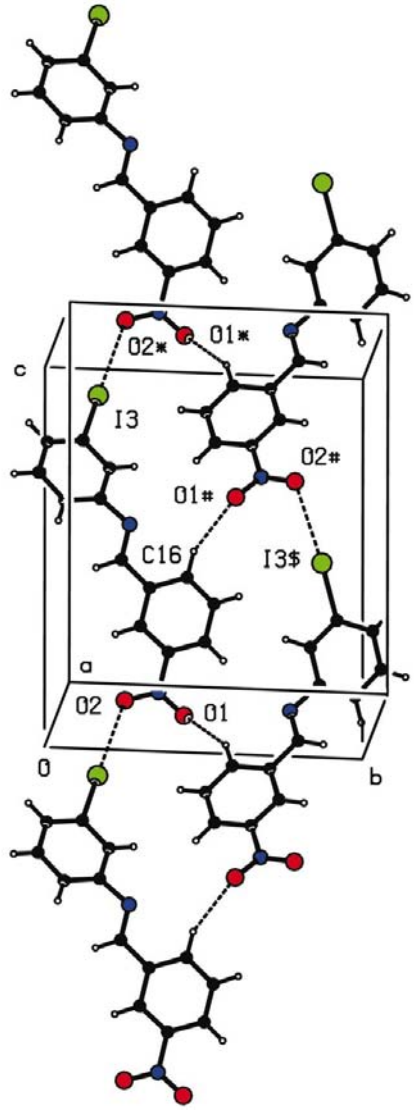

Figure 13
Part of the crystal structure of compound (V), showing the formation of a molecular ladder parallel to [001]. The atoms marked with a star (*), hash (#) or dollar sign ($) are at the symmetry positions $(x, y, 1 + z)$ and $(\frac{1}{2} - x, 1 - y, \frac{1}{2} + z)$ and $(\frac{1}{2} - x, 1 - y, -\frac{1}{2} + z)$, respectively.

A single $\pi\cdots\pi$ stacking interaction links the [001] chains into sheets. The planes of the nitro-arene rings at (x, y, z) and $(1-x, 1-y, 1-z)$ are separated by 3.364 (3) Å: the corresponding centroid separation is 3.644 (3) Å, with a centroid offset of 1.401 (3) Å (Fig. 12). The molecules at (x, y, z) and $(1-x, 1-y, 1-z)$ are themselves components of the two [001] chains generated by the glide planes at $y = 0.75$ and $y = 0.25$, respectively. Similarly, the nitro-arene ring in the molecule at $(x, \frac{3}{2}-y, -\frac{1}{2}+z)$, a component of the $y = 0.75$ chain, forms a $\pi\cdots\pi$ stacking interaction with the corresponding ring in the molecule at $(1-x, \frac{1}{2}+y, \frac{1}{2}-z)$, which is a component of the chain generated by the *c*-glide plane at $y = 1.25$. Propagation of this interaction by the space group links the [001] chains into sheets parallel to (100) but with no direction-specific interactions between neighbouring sheets.

4.3.2. Molecular ladders linked into sheets by $\pi\cdots\pi$ interactions. Compounds (V) and (VI) both crystallize in space group $P2_12_12_1$ with somewhat similar cell dimensions (Table 1), but they are by no means isostructural (Figs. 5 and 6). However, the principal features of their supramolecular structures are very similar: in both compounds, weak C—H···O hydrogen bonds form chains along the [001] direction, generated by the 2_1 screw axis along $(\frac{1}{4}, \frac{1}{2}, z)$, although the chains are of the *C*(7) and *C*(11) types, respectively, involving donor atoms from different aryl rings (Figs. 5 and 6; Table 3); in both compounds, there are two-centre iodo···nitro interactions generating by translation chains parallel to [001] so that the combined effect of the hydrogen bond and the iodo···nitro interaction is the formation in each case of a chain of fused rings or a molecular ladder (Figs. 13 and 14; Table 4). In both compounds, these ladders are linked into (010) sheets by the aromatic $\pi\cdots\pi$ stacking interactions (Figs. 15 and 16). Because of these similarities, we discuss in detail only the structure of (V).

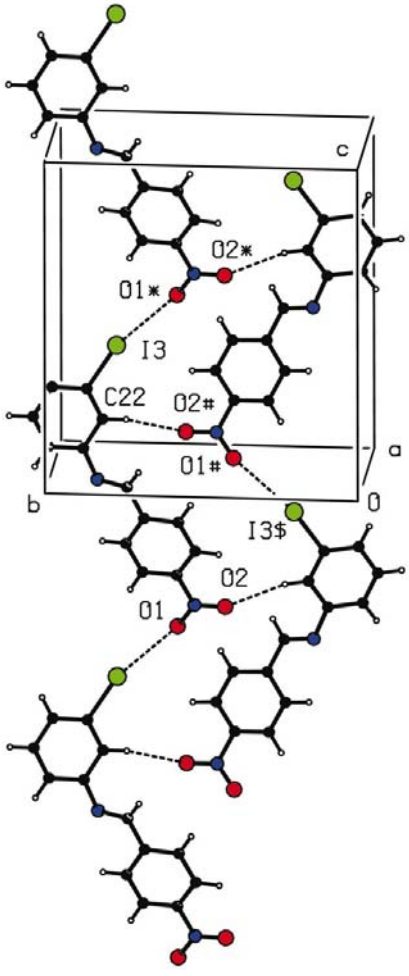

Figure 14
Part of the crystal structure of (VI) showing the formation of a molecular ladder parallel to [001]. The atoms marked with a star (*), hash (#) or dollar sign ($) are at the symmetry positions $(x, y, 1+z)$ and $(\frac{1}{2}-x, 1-y, \frac{1}{2}+z)$ and $(\frac{1}{2}-x, 1-y, -\frac{1}{2}+z)$, respectively.

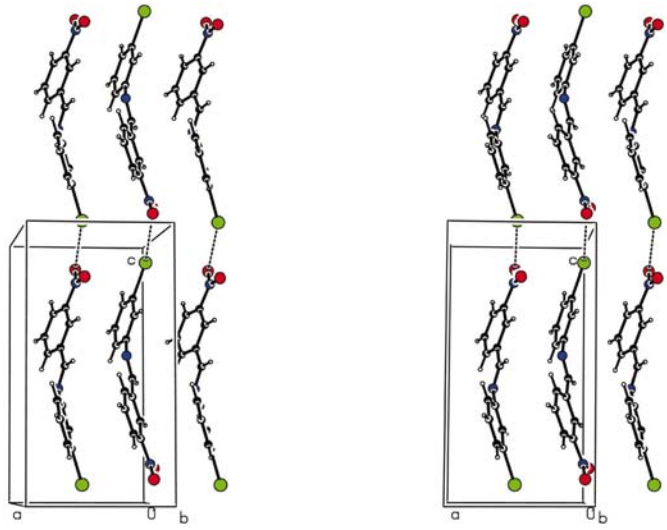

Figure 15
Stereoview of part of the structure of (V) showing the $\pi\cdots\pi$ stacking interactions.

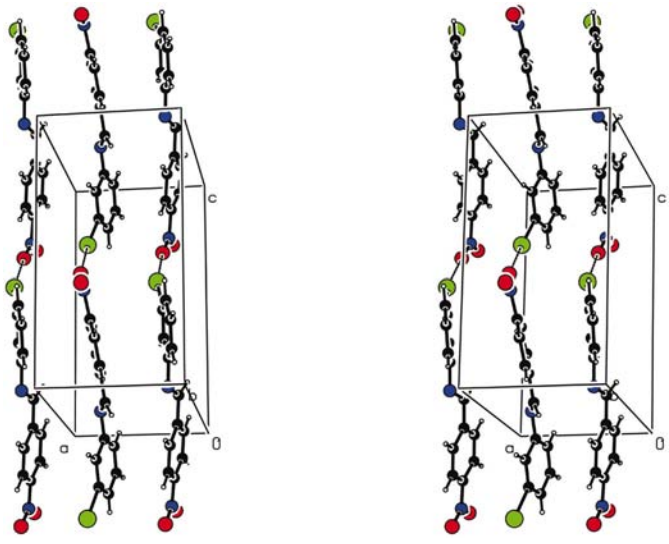

Figure 16
Stereoview of part of the structure of (VI) showing the $\pi\cdots\pi$ stacking interactions.

In (V), I3 in the molecule at (x, y, z) is involved in a two-centre iodo···nitro interaction with O2 at $(x, y, 1 + z)$, so generating by translation a $C(11)$ chain running parallel to the [001] direction. In addition, C16 at (x, y, z) acts as hydrogen-bond donor to O1 at $(\frac{1}{2} - x, 1 - y, \frac{1}{2} + z)$, while C16 at $(\frac{1}{2} - x, 1 - y, \frac{1}{2} + z)$ in turn acts as donor to O1 at $(x, y, 1 + z)$, so producing a $C(7)$ spiral chain along [001]. The combination of the two [001] chain motifs generates a molecular ladder in which the $C(11)$ chains form the uprights and the C—H···O hydrogen bonds form the rungs: between the rungs there are $R_3^3(19)$ rings (Fig. 13). In (VI), the uprights of the ladder are $C(12)$ chains and the rings are of R_3^3 type (Fig. 14).

The aromatic $\pi\cdots\pi$ stacking interactions involve both aryl rings in each of (V) and (VI): molecules related by a 2_1 screw axis parallel to [100] are aligned such that the iodo-arene ring in the molecule at (x, y, z) forms stacking interactions with the nitro-arene rings of the two adjacent molecules. In (V), these are at $(\frac{1}{2} + x, \frac{1}{2} - y, 1 - z)$ and $(-\frac{1}{2} + x, \frac{1}{2} - y, 1 - z)$; the π-stacked rings are inclined at 8.4 (3)° with interplanar separations of 3.374 (4) Å and 3.344 (4) Å and centroid separations of 3.722 (4) Å and 3.834 (4) Å, respectively. In (VI), the interplanar angle between the iodo-arene ring at (x, y, z) and the nitro-arene rings at $(\frac{1}{2} + x, \frac{3}{2} - y, 1 - z)$ and $(-\frac{1}{2} + x, 1.5 - y, 1 - z)$ is 8.3 (3)°, with interplanar separations of 3.458 (3) Å and 3.481 (3) Å and centroid separations of 3.684 (3) Å and 3.719 (3) Å, respectively.

4.3.3. Isolated sheets. Compound (VII) crystallizes in space group $C2/c$ with $Z' = 2$ in a unit cell of rather unusual dimensions and shape (Table 1). The supramolecular structure is characterized by a long two-centre iodo···nitro interaction involving I24 (but not I14) and by C—H···O hydrogen bonds (Tables 3 and 4). Within the asymmetric unit (Fig. 7), atom C13 in the type 1 molecule acts as hydrogen-bond donor to O31 in the type 2 molecule; these two-molecule units are linked by the single iodo···nitro interaction into a chain running parallel to the [001] direction. Atom I24 in the type 2 molecule at (x, y, z) is linked to O12 in the type 1 molecule at $(x, 2 - y, -\frac{1}{2} + z)$, while I24 at $(x, 2 - y, -\frac{1}{2} + z)$ is in turn linked to O12 at $(x, y, -1 + z)$. These two interactions thus produce a $C_2^2(16)$ chain, generated by the c-glide plane at $y = 1.0$ (Fig. 17).

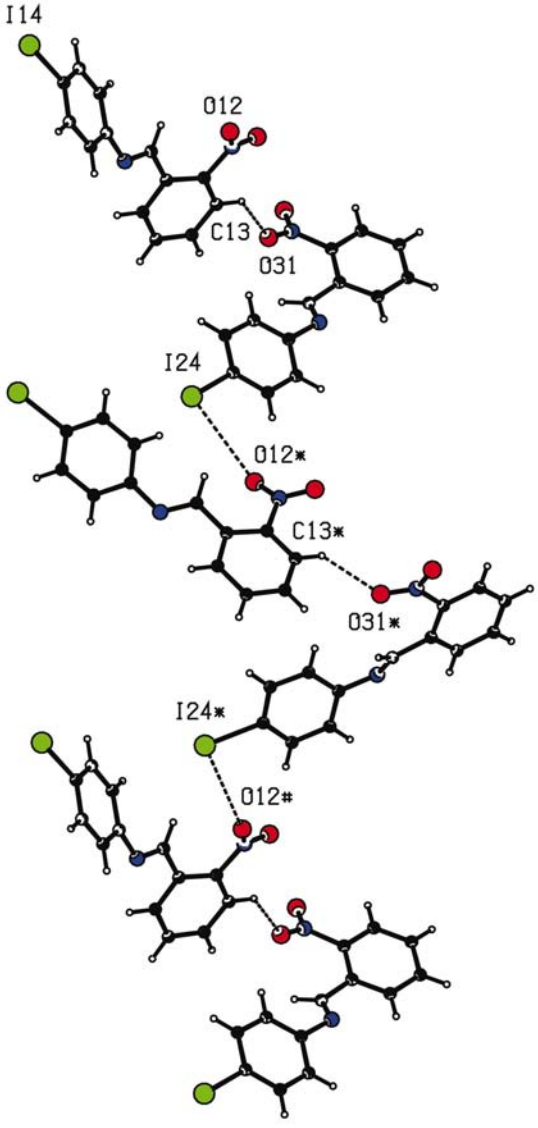

Figure 17
Part of the crystal structure of (VII) showing the formation of a chain along [001]. For the sake of clarity, the unit-cell box is omitted. The atoms marked with a star (*) or hash (#) are at the symmetry positions $(x, 2 - y, -\frac{1}{2} + z)$ and $(x, y, -1 + z)$, respectively.

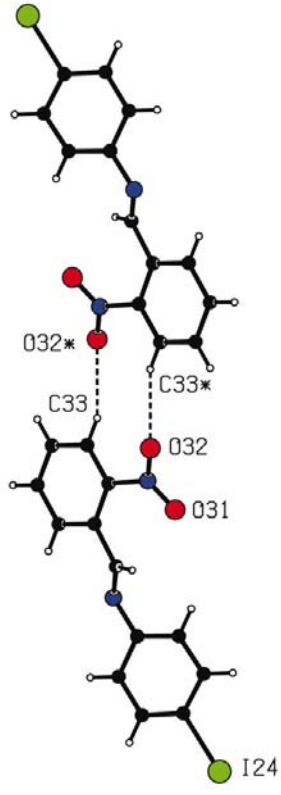

Figure 18
Part of the crystal structure of (VII) showing the formation of an $R_2^2(10)$ ring. For the sake of clarity, the unit-cell box is omitted. The atoms marked with a star (*) are at the symmetry position $(1 - x, -1 - y, 1 - z)$.

In addition to this [001] chain, two further C—H···O hydrogen bonds combine to form a chain of rings running parallel to [010]. C33 in the type 2 molecule at (x, y, z) acts as hydrogen-bond donor to O32 in the type 2 molecule at ($1-x$, $-1-y$, $1-z$), so generating a centrosymmetric $R_2^2(10)$ ring (Fig. 18). Similarly, C34 in the type 2 molecule at (x, y, z) acts as donor to O11 in the type 1 molecule at ($1-x$, $-y$, $1-z$): in combination with the C—H···O hydrogen bond within the asymmetric unit, this generates a second centrosymmetric ring, of $R_4^4(22)$ type (Fig. 19). The propagation by inversion of these two cyclic motifs generates a [010] chain, with the $R_2^2(10)$ ring centred at ($\frac{1}{2}$, $n+\frac{1}{2}$, $\frac{1}{2}$) (n = zero or integer) and the $R_4^4(22)$ rings centred at ($\frac{1}{2}$, n, $\frac{1}{2}$) (n = zero or integer).

The combination of the [010] and [001] chains generates a sheet lying parallel to (100), and there are two such sheets passing through each unit cell, in the domains $0.21 < x < 0.79$ and $0.71 < x < 1.29$: they are related to one another by the C-centring operation, but there are no direction-specific interactions between adjacent sheets.

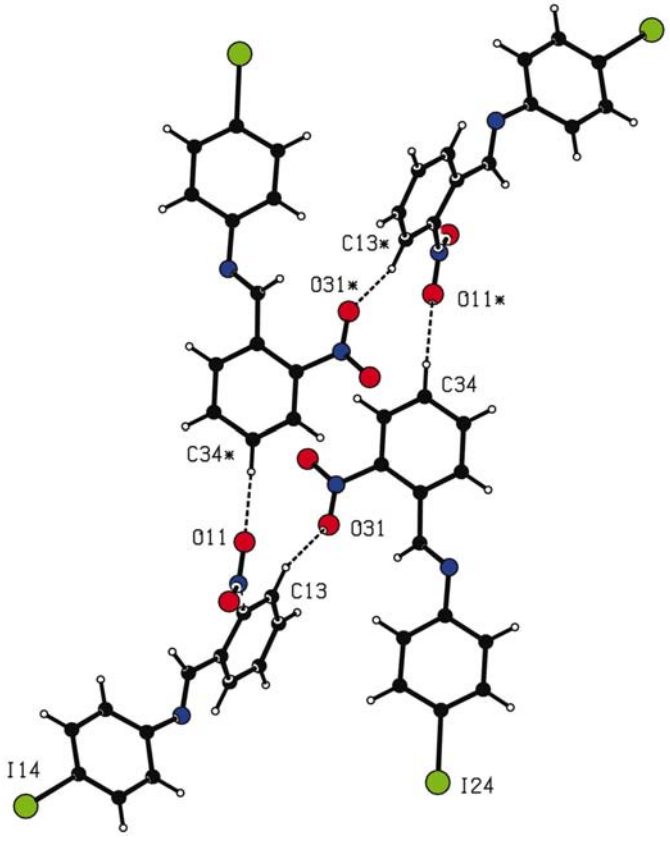

Figure 19
Part of the crystal structure of (VII) showing the formation of an $R_4^4(22)$ ring. For the sake of clarity, the unit-cell box is omitted. The atoms marked with a star (*) are at the symmetry position ($1-x$, $-y$, $1-z$).

4.4. Three-dimensional structures

4.4.1. Sheets linked by $\pi\cdots\pi$ interactions. Compound (VIII) also crystallizes with $Z' = 2$, but in space group $P\bar{1}$, and in contrast to (VII), both of the I atoms participate in short two-centre iodo···nitro interactions. Within the asymmetric unit, there is a C—H···O hydrogen bond (Fig. 8), and in combination with the two I···O interactions this generates a chain of edge-fused rings. Atom I14 in the type 1 molecule at (x, y, z) is linked to O32 in the type 2 molecule at ($2-x$, $-y$, $2-z$), so generating a centrosymmetric $R_4^4(22)$ ring, centred at (1, 0, 1) (Fig. 20). In a similar fashion, I24 at (x, y, z) is linked to O12 at ($1-x$, $2-y$, $1-z$), so generating a centrosymmetric $R_4^4(38)$ ring centred at ($\frac{1}{2}$, 1, $\frac{1}{2}$). Propagation of these motifs by the successive inversion centres generates a chain of rings running parallel to the [$1\bar{2}1$] direction (Fig. 20). This can alternatively be regarded as a molecular ladder in which a pair of antiparallel chains generated exclusively by the iodo···nitro interactions form the uprights, while the rungs are formed by the C—H···O hydrogen bond within the asymmetric unit.

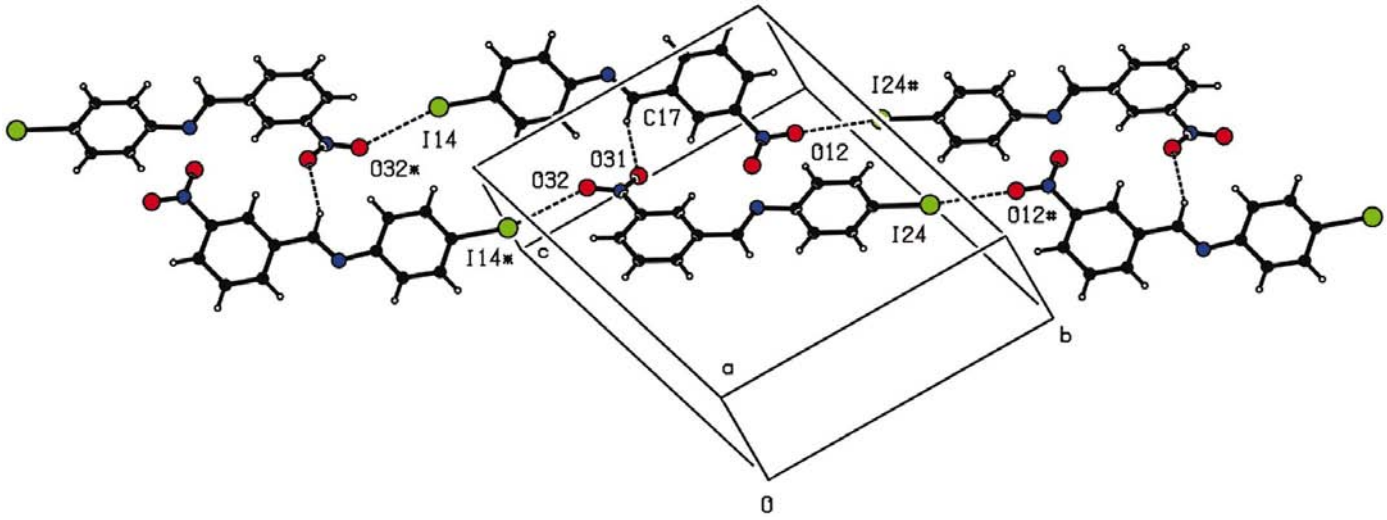

Figure 20
Part of the crystal structure of (VIII) showing the formation of a molecular ladder along [$1\bar{2}1$]. The atoms marked with a star (*) or hash (#) are at the symmetry positions ($2-x$, $-y$, $2-z$) and ($1-x$, $2-y$, $1-z$), respectively.

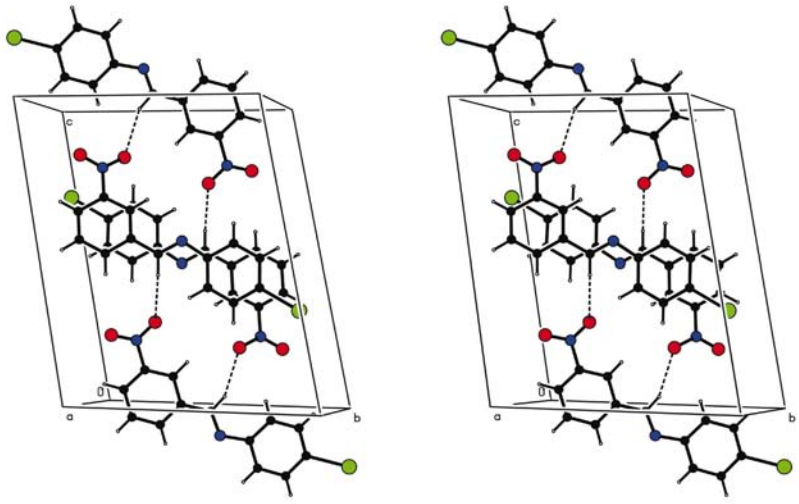

Figure 21
Stereoview of part of the crystal structure of (VIII) showing the formation of the centrosymmetric $R_4^4(28)$ motif that links the molecular ladders into sheets.

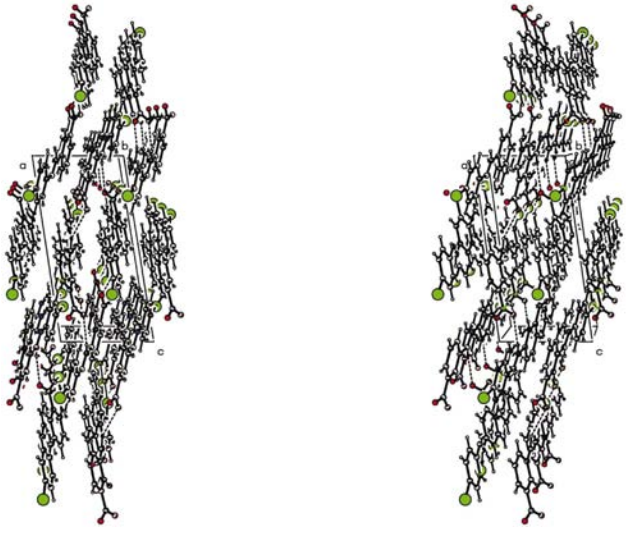

Figure 22
Stereoview of part of the crystal structure of (VIII) showing the formation of a $(10\bar{1})$ sheet.

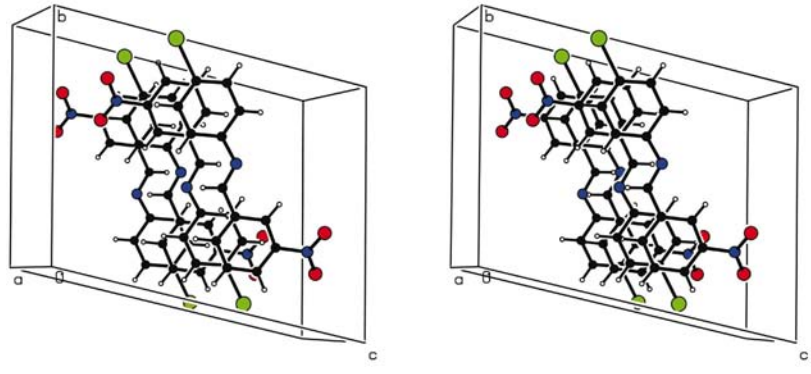

Figure 23
Stereoview of part of the structure of (VIII) showing the $\pi\cdots\pi$ stacking interactions linking the (101) sheets.

The $[1\bar{2}1]$ chains are linked into a (101) sheet by the second C—H···O hydrogen bond, where C37 in the type 2 molecule at (x, y, z) acts as donor to O11 in the type 1 molecule at ($1-x$, $1-y$, $1-z$), so forming an $R_4^4(28)$ ring centred at ($\frac{1}{2}$, $\frac{1}{2}$, $\frac{1}{2}$) (Fig. 21). It will be noted (Fig. 20) that while the C17—H17 bonds all point towards the interior of the $[1\bar{2}1]$ ladder, the C37—H37 bonds are all on the exterior edges, and hence the hydrogen bonds formed by C37 serve to link each such ladder to the two neighbouring ladders, so forming a continuous sheet parallel to $(10\bar{1})$ (Fig. 22).

Adjacent sheets are linked into a single three-dimensional framework by aromatic $\pi\cdots\pi$ stacking interactions. The rings C21—C26 in the type 1 molecule at (x, y, z) and C41—C46 in the type 2 molecule at ($2-x$, $1-y$, $1-z$) lie in adjacent $(10\bar{1})$ sheets. These rings make an interplanar angle of only 4.3 (2)°, with a centroid separation of 3.650 (2) Å and an interplanar spacing of *ca.* 3.40 Å (Fig. 23).

4.5. General comments on the supramolecular structures

A number of patterns can be discerned in the supramolecular structures of (I)–(VIII): it is, of course, unfortunate that no refinable structure solution was possible for (IX).

(*a*) Compounds (VII)–(IX), where the iodo substituent is in the 4′ position, all crystallize with $Z' = 2$. All other compounds in this series crystallize with $Z' = 1$.

(*b*) When the iodo substituent is in the 2′ position [compounds (I)–(III)], iodo···nitro interactions are absent, regardless of the location of the nitro group and of the location of the iodinated ring relative to the central spacer unit. Such interactions are also absent from the structure of (IV).

(*c*) Aromatic $\pi\cdots\pi$ stacking interactions are absent when the nitro group is in the 2 position [compounds (I), (IV) and (VII)]: these interactions are also absent from the structure of (II).

(*d*) Intermolecular C—H···O hydrogen bonds occur in all compounds except (I), but despite the presence of a lone pair at the imino nitrogen there is no evidence for C—H···N hydrogen-bond formation in any of these compounds.

(*e*) Only when neither the iodo nor the nitro substituents are in 2 positions

[compounds (V), (VI) and (VIII)] do all three types of intermolecular interaction manifest themselves.

5. Concluding comments

The crystallization characteristics of nitrobenzylidene-iodoaniline isomers with Z' values of either 1 or 2, the molecular conformations (§3) and the patterns in the supramolecular aggregation (§4), to which might be added those of the 'reverse isomer' 2-iodobenzylidene-3′-nitroaniline [Wardell *et al.* (2002), space group $P\bar{1}$, $Z' = 1$] where the molecules are linked into sheets by a combination of C—H···O hydrogen bonds and $\pi\cdots\pi$ stacking interactions (but not iodo···nitro interactions), all point to a subtle interplay of the weak direction-specific intermolecular forces. Weak forces of the types manifest here, dependent on molecular polarizability and polarization, are not easy to model computationally. The variations in the supramolecular aggregation behaviour within an extended series of isomeric compounds, such as those described here, provides a keen test of computational methods for crystal-structure prediction (Lommerse *et al.*, 2000): the accurate prediction of behaviour across such a series of isomeric species would generate real confidence in the efficacy of the predictive method employed.

X-ray data were collected at the EPSRC X-ray Crystallographic Service, University of Southampton, UK. The authors thank the staff of the service for all their help and advice. JNL thanks NCR Self-Service, Dundee, for grants that have provided computing facilities for this work. JLW and SMSVW thank CNPq and FAPERJ for financial support.

References

Bernstein, J., Davis, R. E., Shimoni, L. & Chang, N.-L. (1995). *Angew. Chem. Int. Ed. Engl.* **34**, 1555–1573.
Domenicano, A., Schultz, G., Hargittai, I., Colapietro, M., Portalone, G., George, P. & Bock, C. W. (1990). *Struct. Chem.* **1**, 107–122.
Etter, M. C. (1990). *Acc. Chem. Res.* **23**, 120–126.
Ferguson, G. (1999). *PRPKAPPA*. University of Guelph, Canada.
Flack, H. D. (1983). *Acta Cryst.* A**39**, 876–881.
Kelly, C. J., Skakle, J. M. S., Wardell, J. L., Wardell, S. M. S. V., Low, J. N. & Glidewell, C. (2002). *Acta Cryst.* B**58**, 94–108.
Lommerse, J. P. M., Motherwell, W. D. S., Ammon, H. L., Dunitz, J. D., Gavezzotti, A., Hofmann, D. W. M., Leusen, F. J. J., Mooij, W. T. M., Price, S. L., Schweizer, B., Schmidt, M. U., van Eijck, B. P., Verwer, P. & Williams, D. E. (2000). *Acta Cryst.* B**56**, 697–714.
Motherwell, W. D. S., Shields, G. P. & Allen, F. H. (1999). *Acta Cryst.* B**55**, 1044–1056.
Nonius (1997). *KappaCCD Server Software*. Windows 3.11 Version. Nonius BV, Delft, The Netherlands.
Otwinowski, Z. & Minor, W. (1997). *Methods Enzymol.* **276**, 307–326.
Sheldrick, G. M. (1997*a*). *SHELXL*97. University of Göttingen, Germany.
Sheldrick, G. M. (1997*b*). *SHELXS*97. University of Göttingen, Germany.
Spek, A. L. (2002). *PLATON*. Version of March 2002. University of Utrecht, The Netherlands.
Starbuck, J., Norman, N. C. & Orpen, A. G. (1999). *New J. Chem.* **23**, 969–972.
Wardell, J. L., Wardell, S. M. S. V., Skakle, J. M. S., Low, J. N. & Glidewell, C. (2002). *Acta Cryst.* C**58**, o428–o430.
Wilson, A. J. C. (1976). *Acta Cryst.* A**32**, 994–996.